Complete Assignment of ^{1}H NMR Spectra and Structural Analysis of Intact Bacteriochlorophyll *c* Dimer in Solution

Zheng-Yu Wang,* Mitsuo Umetsu, Masayuki Kobayashi, and Tsunenori Nozawa

Department of Biomolecular Engineering, Faculty of Engineering, Center for Interdisciplinary Science, Tohoku University, Sendai 980-8579, Japan

Received: November 19, 1998

Intact farnesyl (3^1R)-bacteriochlorophyll (BChl) *c* in carbon tetrachloride forms a stable dimer at room temperature characterized by two resonances resolved for each individual proton in the NMR spectrum and by a long wavelength shift of the Q_y absorption band to 710 nm. All the proton resonances are precisely assigned on the basis of two-dimensional H−C and H−H correlation experiments. Authentic farnesyl acetate is used for assistance in the assignment. Extensive nuclear Overhauser effects (NOE) are observed, from which distances between intermolecular proton pairs are evaluated. Geometry of the macrocycles determined from the distance information and refined by a molecular mechanics program is found to clearly explain the observed complexation shifts. Strong intermolecular NOE signals observed for 10-H/20^1-H and 10-H/2^1-H exclude a face-to-face arrangement but support an antiparallel "piggy-back" conformation for the BChl *c* dimer. Farnesyl protons do not show significant complexation shifts, and it is suggested that the farnesyl side chain may adopt a folding-back conformation with most of the group fluctuating around the periphery of the macrocycle in a restricted motion. The two-dimensional exchange experiment demonstrates that molecules in the dimer experience slow exchange between the two nonequivalent configurations with an exchange rate constant of about 1.8 s^{-1}. Finally, the stereochemical effect of chirality at the 3^1 position on the aggregation behavior and possible relationships among 680, 710, and 740 nm species are discussed.

Introduction

Bacteriochlorophyll (BChl) *c* is a major green pigment family that occurs only in green photosynthetic bacteria. About 90% of the total chlorophyll-type pigments were found as a BChl *c* homologous mixture in green nonsulfur bacteria (Chloroflexaceae) and in many species of green sulfur bacteria (Chlorobiaceae).[1−3] Most BChl *c* is present in chlorosomes, antenna complexes attached to the inner surface of cytoplasmic membrane of the cell. In *Chlorobium tepidum*, the chlorosomes have elongated bodies of uniform shape and size with a typical dimension of 150 nm × 60 nm.[4] They function to absorb light energy, which is then transferred to the adjacent photosynthetic membrane. Because only a small amount of protein was isolated from chlorosomes with a protein to BChl *c* ratio of about 0.5:1 (w/w),[5,6] which is nearly 2- to 3-fold lower than in light-harvesting antenna of other photosynthetic species,[3,7] pigment−pigment interaction has been suggested to play an essential role in the organization of the pigments in chlorosomes.[3,8−11] However, the exact role of the small amount of protein in the chlorosome structure, function, and assembly has remained controversial despite the efforts of many investigators.[12−15]

Apart from the functionality of protein, BChl *c* is capable of self-association in vitro to form various aggregates with different sizes in organic solvents. Purified BChl *c* forms oligomers in hexane with the Q_y absorption peak at ∼740 nm, about 70 nm red-shifted from that of its monomeric form as observed in methanol, and the absorption spectra closely resemble that of BChl *c* in chlorosomes.[16,17] In addition to the 740 nm oligomer, there are at least two other aggregates formed in CH_2Cl_2, $CHCl_3$, and CCl_4 (or benzene) with absorption maxima at 680 and 710 nm for *R*-type BChl *c*.[8,18,19] The 710 nm species is reported to exhibit unusual spectroscopic properties, in particular an intense fluorescence emission.[8,20] A large number of studies have been made to elucidate the structure of the 740 nm aggregate in relation with the organization of BChl *c* in chlorosomes.[8−11,16,17,21−23] Descriptions of the large aggregation structure have converged into two basic models[3] in which the BChl *c* molecules are arranged in antiparallel or parallel chains. In the antiparallel model, molecules in each chain are linked by an H-bond between the 3^1-hydroxyl and 13^1-keto groups, with the BChl *c* in opposite chains being attached by hydroxyl ligation of the central Mg atom, whereas in the parallel model, each BChl *c* molecule is linked to the next by 3^1-hydroxyl-to-Mg ligation and to the one after the next by 3^1-hydroxyl-to-13^1-keto H-bonding. Nozawa et al.[9,10] extended the antiparallel chain model, known as the "ring overlap model", and included more than a single row of pigments in the oligomer. Chiefari et al.[11] proposed an extension of the parallel chain model that also includes more than two chains of pigments. However, owing to the large molecular weight and structural inhomogeneity, the structure of the 740 nm aggregates has not been solved.

With the difficulties in determining the structure of 740 nm aggregates, the intermediate 680 and 710 nm oligomers have attracted the attention of researchers with speculation that these oligomers may serve as building units of the 740 nm aggregates. A detailed study of the structure of an oligomer closely related to BChl *c* was first made by Smith et al.[24] for bacteriochlorophyllide (BChlide) *d*, which differs from BChl *c* at the 20-carbon with the methyl group (BChl *c* only, Figure 1) replaced by a proton and with the farnesyl chain replaced by a methyl group. The BChlide *d* oligomer in pure $CDCl_3$ has been definitely

* To whom correspondence should be addressed. Phone/Fax: +81-22-217-7278. E-mail: wang@biophys.che.tohoku.ac.jp.

10.1021/jp984483t CCC: $18.00
Published on Web 04/20/1999

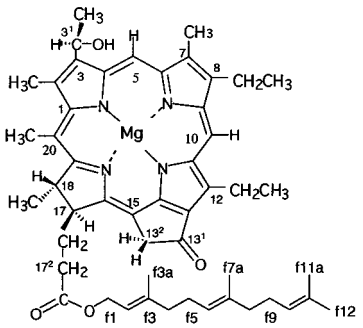

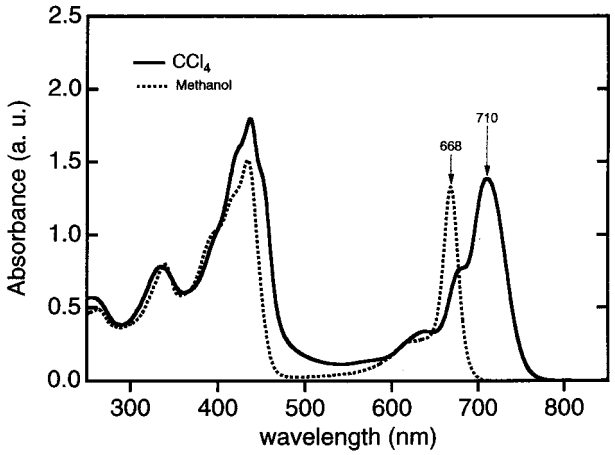

Figure 1. Molecular structure of the intact (3[1]*R*)-[*E*,*E*]-BChl c_F and its absorption spectra in pure CCl_4 (solid line) and in methanol (dotted line). Both concentrations were 2 mM.

shown by proton NMR spectroscopy to be a stable dimer that is long-lived on the NMR time scale. Two possible structures, known as "face-to-face" and "piggy-back" models, were shown to be consistent with the observed chemical shifts based on a double-dipole ring current calculation.[25,26] Similar structures have been proposed for BChl *c* in $CDCl_3$ because of the similarity of the spectra.[9,24] The 680 and 710 nm species are considered to exist at equilibrium, since the two species almost always appear together and their absorption intensities are dependent on the total BChl *c* concentration and polarity of the solvents. Olson and Cox[19] propounded the aggregation state of the 710 nm species to be a tetramer formed by association of two dimers from the concentration dependence of absorption spectra. However, Causgrove et al.[20] proposed a cyclic arrangement of three dimers for the 710 nm species from the result of polarized fluorescence experiments, and they argued that this species is probably not a building block of the large aggregates. In a previous paper, we have definitely demonstrated that the 710-nm-rich species is predominated by BChl *c* dimers on the basis of small-angle neutron scattering experiments from which the sizes of aggregates were determined without using fitting parameters.[27]

In this study, we present detailed assignment of ^{1}H NMR spectra of intact BChl *c* dimer in pure CCl_4 solution made by two-dimensional heteronuclear and homonuclear correlation techniques. The sample used is (3[1]*R*)-[*E*,*E*]BChl c_F (8,12-diethyl BChl *c* esterified with farnesol), the most abundant component constituting about 70% of whole BChl *c* homologues[28] and showing a 710 nm absorption maximum in CCl_4 solution (Figure 1). Our reason for using the intact BChl *c* is that it has been suggested that the farnesyl chain plays an important role in the aggregation of BChl *c* with the ester carbonyl group engaged in strong hydrogen bondings as revealed by NMR,[24] FT-IR, and FT-Raman experiments.[29] Authentic farnesyl acetate was used to assist identification of the farnesyl proton resonances. The spectra recorded for the 710 nm species can be best interpreted in terms of a physically exchanging dimer with a characteristic feature of asymmetric conformation. Analyses of the structure and dynamics of the dimer are made based on the results of two-dimensional nuclear Overhauser enhancement and exchange (NOESY) and rotating frame nuclear Overhauser effect (ROESY) experiments. Quantitative measurement of the extensive NOE signals allows a precise evaluation of the dimer structure and dynamics without relying on specific models. The results of this study confirm and emphasize many of the previous findings and provide independent evidence for the intermolecular distance and macrocyclic geometry. A recent X-ray crystallographic study by Senge and Smith[30] on the methyl ester of (20-methylphytochlorinato)nickel(II), an analogue of BChl *c*, demonstrated a higher degree of conformational distortion of the macrocycle at the methyl-substituted C20 position compared with BChl *d* series. Existence of the methyl group at C20 has been found to be responsible for a 10 nm red shift of the long wavelength absorbing band in ether and a 20 nm red shift in living cells.[31,32] In this respect, our result may provide complementary information for clarifying the structural and functional differences between the BChl *c* and the BChl *d* series.

Experimental Section

Materials and Sample Preparation. Crude BChl *c* mixtures were extracted from dry cells of *Chlorobium tepidum* with methanol, and the major component (3[1]*R*)-[*E*,*E*]-BChl c_F was then purified by chromatography as described elsewhere.[9,10] A partially ^{13}C-labeled sample was obtained by a similar procedure except that the sodium acetate in the culture medium was replaced by sodium acetate-1-^{13}C (^{13}C > 99.9 atom %, Isotec Inc.). Farnesyl acetate (*trans*,*trans*-, purity > 95%) was purchased from Aldrich Chem. Co. (Milwaukee, WI). Deuterated methanol (CD_3OD, D > 99.95%) was from Merck (Darmstadt, Germany). Carbon tetrachloride (purity > 99.8%, Infinity pure grade) was purchased from Wako Pure Chemical Industries, Ltd. (Japan) and was dried with Na_2CO_3 during storage. Pigments and solvents were degassed separately and then purged with argon gas; this operation was repeated several times. BChl *c* solutions were prepared under an argon atmosphere by dissolving the dried pigments in solvents with a monomer concentration of 2 mM. The solutions were then moved into NMR tubes and further purged with argon gas before sealing the NMR tubes.

NMR Measurements. All NMR experiments were acquired on a Bruker DRX-400 spectrometer equipped with an inverse probe (TXI) and gradient module. Temperature was controlled at 22 °C by a Bruker variable-temperature controller. Field-frequency lock for the sample in pure CCl_4 solution was achieved by inserting a 1 mm D_2O-filled inner tube in the 5 mm NMR tubes. One-dimensional ^{1}H spectra were recorded with 32K data points, sweep width of 5827 Hz giving a digital resolution of 0.35 Hz/point, acquisition time of 2.8 s, and 64 accumulations. Two-dimensional ^{1}H−^{1}H spectra were acquired with a spectral width of 5500 Hz, 512 t_1 points, 2K data points in t_2, and 16, 24, or 32 transients for each t_1 point. Double quantum filtered (DQF) COSY spectra were performed using the pulse sequence described by Davis et al.,[33] in which the phase information during the evolution period is retained and a

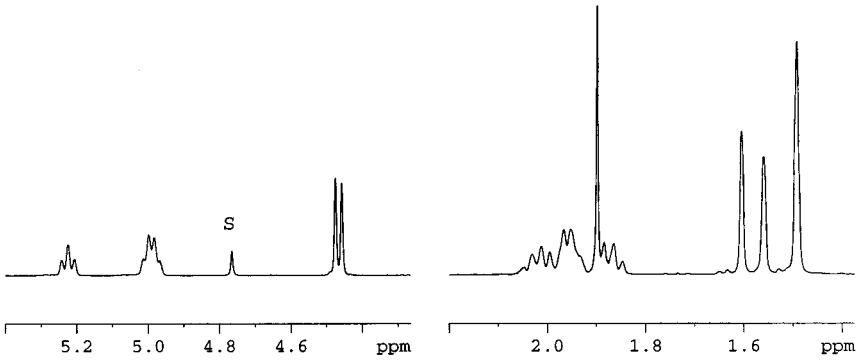

Figure 2. ^{1}H NMR spectrum of authentic *trans,trans*-farnesyl acetate in methanol at concentration of 10%. Peak marked S is due to nondeuterated methanol impurities in the solvents.

phase-sensitive spectrum with pure absorption line shapes is produced. Gradient pulses were present only during the double quantum period and just prior to acquisition. Conventional pulse sequences were used for NOESY and ROESY experiments.[34,35] NOESY spectra were recorded with mixing times of 0.075, 0.15, 0.4, and 1 s. ROESY spectra were recorded with a spin-locked period of 200 ms. Two-dimensional ^{1}H−^{13}C shift correlation spectra using ^{1}H-detected heteronuclear multiple-quantum coherence via a direct coupling method (HMQC) were acquired with the pulse sequence described by Hurd and John.[36] The spectral width for ^{1}H was 4800 Hz and for ^{13}C was 17 kHz. A total of 512 t_1 points of 2K data points were acquired. For each t_1 value 64 or 128 transients were recorded, the number of scans depending on the experiment. During acquisition, the ^{13}C was decoupled using a broadband GARP modulation.[37] Chemical shifts were referenced to tetramethylsilane (TMS). All two-dimensional spectra were recorded in pure absorption with time-proportional phase incrementation (TPPI)[38] to allow for discrimination between positive and negative signals.

Molecular Mechanics Calculation. Molecular mechanics calculations were performed using a HyperChem software (Hyper Cube Co.) on a Indy workstation (Silicon Graphics Inc.). In the calculation, the farnesyl side chain was replaced by an ethyl group. Dimer geometry was optimized using molecular mechanics program MM+ with an extension of force field of MM2 developed by Allinger and co-workers.[39] MM+ treats bond and bond angle terms with higher order terms than the standard quadratic and contains a stretch−bend cross term. Electrostatic potential energy terms were neglected because it was reported to have only a small effect on the structure.[40] Instead, the electrostatic contribution was evaluated by a set of bond dipole moments associated with polar bonds. Distances evaluated from NOESY experiments were employed as restraints in the energy minimization calculation. The force constant used for the strength of the restraints was 700 kcal mol^{-1} Å^{-2}.

Results

Assignments of Farnesyl Acetate. Figure 2 shows the ^{1}H NMR spectra of *trans,trans*-farnesyl acetate in CD_3OD. Eleven resonances out of 13 nonequivalent proton resonances were resolved. Assignments for each proton can be readily made with assistance of DQF-COSY and HMQC spectra, and the results are shown in Table 1. Carbon−carbon connectivity was established by a C−C correlation experiment.[41] The most downfield ^{1}H signal was assigned to be f2-H on the basis of its strong correlation with f1-H. Small splittings (1.1 Hz) were observed for the f2-H triplet, indicating a long-range coupling ($^4J_{trans}$). Resonances of f6-H and f10-H cannot be distinguished from the 1D spectrum owing to structural similarity. However,

TABLE 1: Assignments of *trans,trans*-Farnesyl Acetate in Methanol-d_4

	^{1}H	
position	chemical shift (ppm)	spin coupling[a]
f2-CH	5.223	7.5 (t)
f6-CH	4.998	5.7 (t)
f10-CH	4.983	5.7 (t)
f1-CH_2	4.466	7.1 (d)
f5-CH_2	2.012	6.8 (t)
f4-CH_2	1.963	5.7 (t)
f9-CH_2	1.960	5.7 (t)
f8-CH_2	1.865	7.1 (t)
f3a-CH_3	1.605	(s)
f12-CH_3	1.560	(s)
f11a-CH_3	1.493	(s)
f7a-CH_3	1.493	(s)
CH_3−COO	1.898	(s)

[a] Abbreviations in parentheses: d, doublet; s, singlet; t, triplet. Multiplicities represent the first-order couplings observed from the spectra rather than those predicted from the molecular structure. Values indicate coupling constants in Hz.

the results of H−H and H−C correlation suggest the upfield triplet to be f10-H on which the $^4J_{HH}$ coupling was also observed. Among the four CH_2 groups (f4, f5, f8, and f9) with chemical shifts in the range 1.8−2.1 ppm, f8 protons were found to give the most upfield resonance from H−C correlation, and the structurally similar f8-H and f9-H yielded almost identical shifts. Resonance of f3a−H was specifically identified by its correlation with f1-H. The H−C correlation spectrum indicated a chemical shift of 1.560 ppm for f12-H, while protons of f7a-H and f11a-H did not yield individual resonances.

Assignments of Intact [*E,E*]-BChl c_F Dimer. Using the assignment of farnesyl acetate, we are able to specifically assign all proton resonances of the intact BChl *c* dimer formed in pure CCl_4. Figure 3a shows that upon formation of dimers the ^{1}H NMR spectrum changed significantly from that of monomers in methanol (Figure 3b), and apparently, there was no simple connection between the two spectra. Each individual proton gave rise to two resonances, yielding a total of 58 signals (parts of them were overlapped) from the 29 nonequivalent protons of each [*E,E*]-BChl c_F molecule (17 attached to macrocycle and 12 to the farnesyl chain). The asymmetric feature of the dimer spectrum is very similar to that observed for BChlide *d* in pure chloroform by Smith and co-workers.[24] Despite the complexity of the ^{1}H spectrum of the [*E,E*]-BChl c_F dimer, fortuitously ^{13}C chemical shifts of the dimers remained almost unchanged, or only slightly changed, with respect to those of the monomer except for peak splittings.[41] This greatly assists the assignment of the ^{1}H spectrum of the dimers through H−C correlation, since the ^{13}C chemical shifts of monomeric species have been well

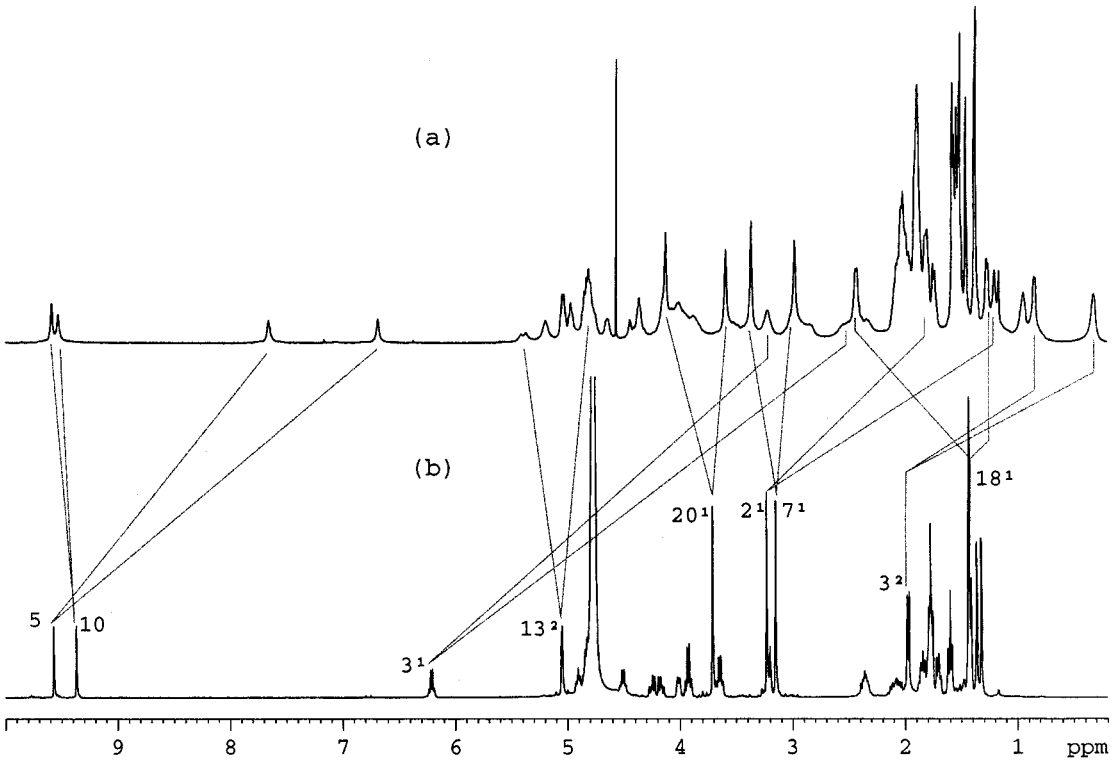

Figure 3. ^{1}H NMR spectra of the intact (3^1*R*)-[*E*,*E*]-BChl c_F (2 mM) in pure CCl_4 (a) and in methanol (b). Peaks marked S are due to nondeuterated water in the inner capillary and nondeuterated methanol in the solvent. Some remarkable shift changes for the key functional groups upon dimer formation are indicated by gray lines. For a full assignment, see Table 2 and text.

established for many chlorophyll derivatives.[22,41−50] Figure 4 shows the H−C correlation spectrum of natural abundance [*E*,*E*]-BChl c_F in CCl_4. When it was combined with the results obtained with the partially ^{13}C-labeled sample, ^{1}H chemical shifts of the [*E*,*E*]-BChl c_F dimer were determined, and the full assignments are given in Table 2.

Assignments of 5-, 10-, and 3^1-H of the dimer spectrum were straightforward, since these protons attach to the carbons whose chemical shifts have been well established. The chemical shifts of the 3^1-H in dimer, heavily overlapped with those of 18^1 and propionic protons (17^1 and 17^2), were also confirmed by their correlations with 3^2-H in the DQF-COSY spectrum. The resonances of 5-H and 3^1-H shifted to higher field and showed the largest complexation shifts ($\Delta\delta = \delta_{dimer} - \delta_{monomer}$), while the resonances of 10-H moved slightly to lower field. This is a typical example demonstrating that the two types of protons in the dimer experienced opposite effects of ring current. Assignment of the 13^2-protons was most difficult because the signals were too weak to be resolved with the natural abundance sample even by long-time acquisition. Use of the partially ^{13}C-enriched sample revealed two pairs of resonances separated by about 0.63 ppm on the ^{1}H-axis and with almost identical ^{13}C chemical shift in the H−C correlation spectrum (Figure 5). Because a strong H−H correlation of an AM coupling pattern was also observed for these protons from the DQF-COSY spectrum (Figure 5), each pair of the resonances can only be interpreted in terms of a doublet, rather than two singlets, with a coupling constant of about 18 Hz. This value is consistent with geminal couplings of five-membered ring compounds with a π-electron system adjacent to the CH_2 group.[51] Large complexation shifts were observed for the 2^1-methyl protons in the dimer spectrum, as can be expected from its proximity to ring I. Four protons on the propionic side chain of each monomer, forming a four-spin system due to chiral centers at 17^1 and 17^2 carbons,[52,53] gave rise to eight well-resolved spots on the dimer HMQC spectrum, but it was not possible to determine the coupling constants. Protons of the 18^1-methyl were assigned on the basis of both H−C correlation and 1D ^{1}H spectral shape, since the two signals can still be clearly observed as doublets in the CCl_4 solution. It was of interest to note that the complexation shifts exhibited a very asymmetric behavior with one shifted to a little higher field and another shifted largely to a lower field. This result provides critical criteria for examining the dimer structure, as will be mentioned in the Discussion. In a similar way, another pair of doublets upfield were assigned as 3^2-methyl protons.

For the farnesyl chain, only f1-methylene showed a single resonance in the dimer spectrum, while two resonances were observed for each of all other groups. The complexation shifts for these protons were relatively small (typically in the range 0.15−0.3 ppm) compared with those of the groups attached to macrocycle, but all had positive values (to the lower field). The protons attached to the backbone of the farnesyl chain had slightly larger complexation shifts than the methyl protons.

NOE Measurements and Exchange Property of [*E*,*E*]-BChl c_F Dimer. It is our aim to obtain information on the geometry and dynamic property of the BChl *c* dimer in solution by NMR. For this purpose, cross-relaxation experiments were conducted. Figure 6 shows the NOESY spectrum of [*E*,*E*]-BChl c_F in CCl_4 with a mixing time of 150 ms. Extensive cross correlation signals with a negative sign (corresponding to negative NOE) were observed in contrast to the positive NOE observed in methanol solution. From the chemical shift assignment of the dimer spectrum, we were able to assign all the signals in terms of either dipole interaction or exchange between the two molecules in the dimer species. Since all signals in the NOESY spectrum had the same sign (negative), further ROESY experiments were carried out to distinguish between the real NOE cross-peaks from those due to exchange, since NOE in the rotating frame is always positive. Figure 7 shows the negative part of the ROESY contour plot in which the

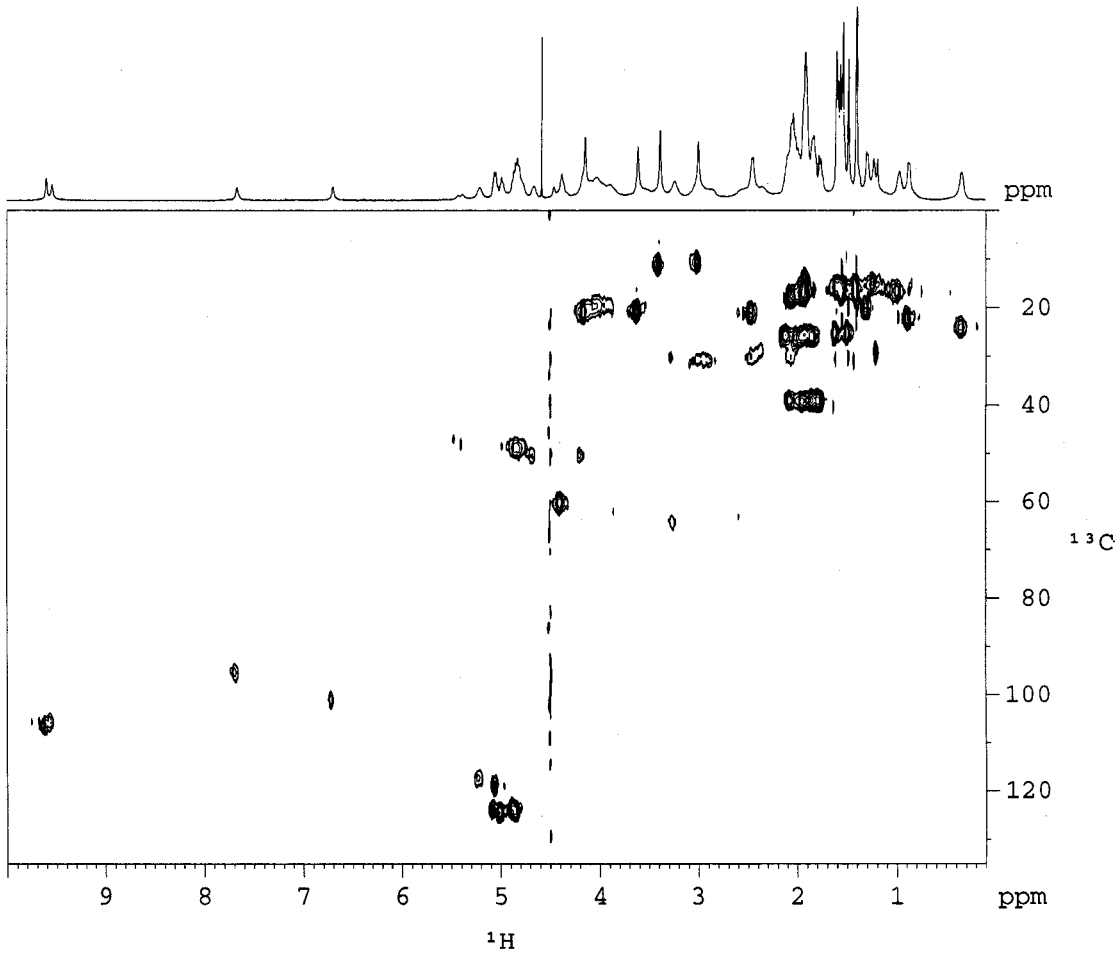

Figure 4. ^{1}H−^{13}C HMQC spectrum of natural abundance (3^{1}*R*)-[*E*,*E*]-BChl c_F (2 mM) in pure CCl_4. For each t_1, 128 transients were recorded. The long thin spots along 4.5 ppm of ^{1}H axis are due to t_1 noise.

resonances have the same phase as diagonal resonances; i.e., all cross-peaks visible are due to exchange. It is evident that physical exchanges occurred for each corresponding proton pair with different configurations. A cross-signal at 4.46 ppm correlated with H-5 was also clearly observed, implying the existence of an exchangeable proton with the meso proton. There is some evidence, from HMQC experiments, that no H−C correlation was found for this proton, and this may be a 3^{1}-hydroxyl proton. After the cross-peaks due to exchange were identified, all other cross-signals can be analyzed in terms of either intramolecular or intermolecular interactions. By comparison with the NOESY spectrum of monomeric [*E*,*E*]-BChl c_F in methanol-d_4, a number of the cross-signals that can only be interpreted by the intermolecular dipole couplings were extracted and listed in Table 3. Clear NOE correlations observed for 10-H/20^{1}-H and 10-H/2^{1}-H strongly suggest a piggy-back (both molecules are in the same orientation with the upper side of one facing the lower side of another[24]), rather than face-to-face, configuration of the dimer.

To evaluate distances from the NOE data, a series of NOESY spectra were recorded with various mixing time, τ_m. Figure 8 shows the integrated intensities of several selected cross-peaks and a diagonal peak as a function of τ_m. The mixing times giving rise to maximum intensities of cross-peaks were found in the range 0.2−0.4 s. Therefore, the relative cross-peak intensities measured with $\tau_m = 0.15$ s can be used to obtain the quantitative distance information with good accuracy on the basis of the initial rate approximation.[54] In this case, an internuclear distance, r_{ij}, can be calculated from the r^{-6} dependence of NOE_{ij} by $r_{ij} = r_0(NOE_0/NOE_{ij})^{1/6}$, where NOE_0 is a measured NOE intensity and corresponds to a known fixed internuclear distance r_0. We choose the average distance of an intramolecular proton pair, 5-H/7^{1}-H as $r_0 = 2.89$ Å and assume that this distance does not change upon dimer formation. Then the intermolecular distances between other proton groups were determined as shown in Table 3. These values were subsequently used as constraints in the molecular mechanics calculation for constructing the [*E*,*E*]-BChl c_F dimer structure.

Determination of the Dimer Structure. The six intermolecular distances determined from NOE experiments imposed strong geometric restriction on the macrocycle configuration. The final dimer structure was refined using the molecular mechanics program MM+. Figure 9 shows two side views of the dimer structure of macrocycles. The farnesyl side chain was replaced by an ethyl group. The 10-proton of the top molecule was located around the upper center between 2^{1}-H and 20^{1}-H of the bottom molecule (Figure 9, top). Consistent with the X-ray crystallographic result,[30] the 20^{1}-methyl group was found to have a large displacement above the macrocyclic mean plane and therefore was closer to 10-H of the upper molecule compared with the 2^{1}-methyl group. The two macrocyclic planes were almost parallel with a separation of about 3.3 Å. From another angle of the side view (Figure 9, bottom), one can see that the 18^{1}-methyl group of the upper molecule points toward the periphery of the macrocycle of the lower molecule with proximity to 3^{1} and 7^{1} protons, whereas the other 18^{1}-methyl group of the lower molecule points away from the dimer moiety. This piggy-back geometry can reasonably explain the asym-

TABLE 2: Assignments of ^{1}H NMR Spectra of Intact [*E*,*E*]-BChl c_F

position	CD_3OD	CCl_4[a]	complexation shift
5-CH	9.572	7.65, 6.68	−1.92, −2.89
10-CH	9.369	9.58, 9.52	0.21, 0.15
3^1-CH	6.215	3.21, 2.53	−3.01, −3.69
13^2-CH_2	5.058	5.395 (J = 18.6)	0.34
	5.050	4.768 (J = 18.2)	−0.28
f2-CH	4.911	5.22, 5.06	0.31, 0.15
f6-CH	4.874	5.08, 4.88	0.21, 0.01
f10-CH	4.829	5.00, 4.85	0.17, 0.02
18-CH	4.511	4.80, 4.76	0.29, 0.25
f1-CH_2	4.210	4.35	0.14
17-CH	4.018	4.63, 4.17	0.61, 0.15
12^1-CH_2	3.931	3.99, 3.88	0.06, −0.05
20^1-CH_3	3.714	4.12, 3.59	0.41, −0.12
8^1-CH_2	3.650	3.99, 3.88	0.34, 0,23
2^1-CH_3	3.232	1.20, 1.87	−2,03, −1.36
7^1-CH_3	3.152	3.36, 2.98	0.21, −0.17
17^2-CH_2	2.36	3.21, 2.98	0.85, 0.62
		2.90, 2.81	0.54, 0.45
17^1-CH_2	2.07	2.40, 2.34	0.34, 0.27
		2.02, 2.00	0.05, 0.07
3^2-CH_3	1.977	0.85, 0.32	−1.13, −1.66
f5-CH_2	1.849	2.09, 1.87	0.24, 0.02
f4-CH_2	1.788	2.04, 1.81	0.25, 0.02
12^2-CH_3	1.777	1.94, 0.95	0.16, −0.82
f9-CH_2	1.758	1.99, 1.80	0.23, 0.04
f8-CH_2	1.704	1.92, 1.73	0.22, 0.03
8^2-CH_3	1.604	2.01, 1.88	0.41, 0.28
f12-CH_3	1.436	1.58, 1.46	0.14, 0.02
f3a-CH_3	1.436	1.57, 1.52	0.13, 0.02
18^1-CH_3	1.417	2.43, 1.27 (J = 5.7), (J = 5.0)	1.01, −0.15
f11a-CH_3	1.368	1.54, 1.38	0.17, 0.01
f7a-CH_3	1.327	1.52, 1.38	0.19, 0.05

[a] Coupling constants are in Hz.

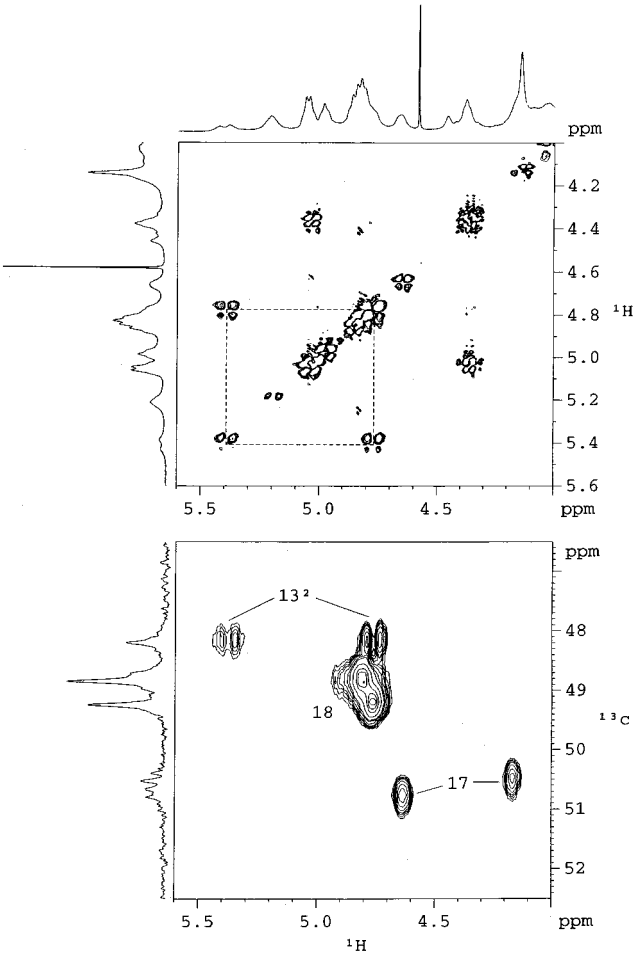

Figure 5. DQF-COSY spectrum of natural abundance (3^1R)-[*E*,*E*]-BChl c_F (top) and ^{1}H−^{13}C HMQC spectrum of partially ^{13}C-labeled (3^1R)-[*E*,*E*]-BChl c_F (bottom) in pure CCl_4 used for the assignment of 13^2 protons. Both samples had a pigment concentration of 2 mM. From the spectra, the geminal coupling constant was determined to be 18 Hz. ^{13}C chemical shifts were assigned on the basis of distortionless enhancement by polarization transfer (DEPT) experiment.[41]

metric behavior observed in the chemical shifts of 18^1-H, for which the complexation shifts were 1.01 and −0.15 ppm, respectively. According to the structure, the hydroxyethyl group is arranged in such a way that the 3^1 proton lies on the same level of the mean plane and the 3^1-hydroxyl group orients toward the central Mg of the adjacent molecule as a ligand while the 3^2-methyl group points to the outside of the dimer. The conformation accounts for the observed large complexation shifts for the 3^1 proton (−3.01 and −3.69 ppm) and small complexation shifts for 3^2 protons (−1.13 and −1.66 ppm). Figure 10 shows a top view of the macrocycles. The overlapping region covers full ring I and a small part of ring II and is much larger than that calculated for the BChlide *d* dimer. As a result, whole 3-hydroxyethyl, 5-H, and 2^1-methyl groups fall inside the macrocycle of the adjacent molecule, resulting in the significant upfield shifts for these protons, whereas for each of the 7^1- and 20^1-methyl pairs, one was located over the boundary of the overlapping area and another located away from the area, consistent with the observed shift behavior. Oxygen atoms of the hydroxyethyl group were found in positions displaced from the vertical about the central Mg of the neighboring molecule. The angle between two Q_y transition moments was measured to be 26.1°.

Discussion

Two-dimensional NMR spectroscopy provides a complementary method to titration experiments and selective labeling by chemical synthesis for the assignment of the complicated dimer spectrum. H−C correlation is particularly useful for assigning those protons with exactly overlapping ^{1}H chemical shifts. The assignments of this study were also greatly facilitated by comparison with the spectrum of authentic farnesyl acetate. Overall, the proton chemical shifts determined for the intact [*E*,*E*]-BChl c_F dimer were in accordance with those for BChlide *d* by Smith et al.[24] but revealed more detail. Previously, only one resonance was tentatively assigned for the 3^1-H at about 2.5 ppm in the BChlide *d* dimer spectrum. We confirmed this assignment by HMQC experiments and further definitely identified another resonance at 3.21 ppm, which totally overlapped those of the side chain propionic protons. The latter assignment is in good agreement with the calculated chemical shift for a piggy-back conformation from the ring current model that predicted a value of 3.5 ppm.[24] Two hydroxyl protons have not been identified in the previous experiment. An unassigned peak at 4.46 ppm of this study was found in correlation with 5-H from the 2D exchange spectrum, and this proton appeared not to bond with a carbon atom. Since the meso protons in chlorophyll and related compounds are known to undergo deuterium exchange with CH_3OD in carbon tetrachloride solution,[47,55] this peak may be assigned as one of the 3^1-hydroxyl protons.

Notably all the resonances for the 13^2 protons in the dimer spectrum have been precisely assigned. We are interested in these protons because they are the most distant from ring I, where the two pyrrole rings are apparently overlapping, and

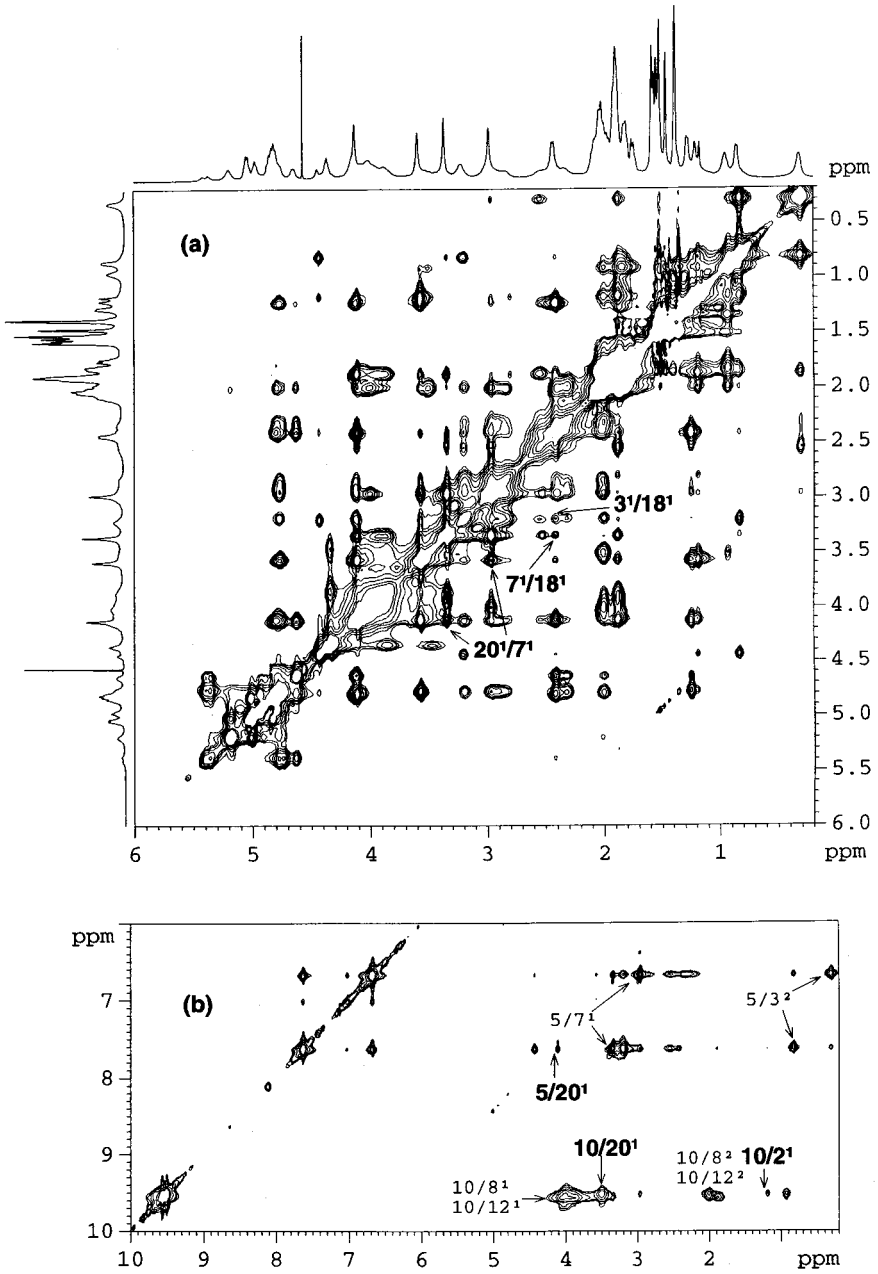

Figure 6. NOESY spectrum of intact (3^1R)-[*E*,*E*]-BChl c_F in pure CCl_4 focused on upfield area (a) and downfield area (b) with a mixing time of 150 ms. For each t_1, 24 transients were recorded. Both diagonal and cross-peaks appeared as a negative phase. Several signals that can only be interpreted by intermolecular dipole couplings are labeled with bold letters, whereas some signals that can be attributed to intramolecular dipole couplings are labeled with plain letters.

could be used as a sensitive probe for examining the ring current effect. The two nonequivalent protons in each molecule became much more distinguishable upon formation of dimer in CCl_4 and resulted in two clearly separate chemical shifts with a geminal coupling constant of 18 Hz (Figure 5). By analogy with chlorophyll *a* and chlorophyll *a*′,[56] the downfield signal may be assigned as the proton above the macrocyclic plane and the other below the plane. In the dimer, the 13^2 protons *above* (or *below*) the nodal planes gave exactly the identical chemical shift for different molecules, indicating that the corresponding protons in different molecules are in the same environment. These protons are the only ones attached to the macrocycle, which show one resonance in the dimer spectrum. It was not clear before whether the change in the chemical shift of 13^2 protons was a direct result of the influence from the adjacent molecules as in the case for other protons. The result of this study indicates that these protons are not affected by the ring current effect from the neighboring macrocycles and that the chemical shifts in the dimer spectrum reflect their intrinsic values of monomer, as a result of the reduced molecular motion (due to increased molecular weight and viscosity). The monomeric behavior of the 13^2 protons may also be considered as evidence showing that the 710 nm species in CCl_4 are composed of uniform [*E*,*E*]-BChl c_F dimers, rather than large oligomers, in which there is no essential macrocycle overlap on ring V.

Compared to the peripheral protons, few remarkable features have been found in the complexation shifts of farnesyl protons. Only f1 protons gave a single resonance in the dimer spectrum, and this may be attributed to their distant position from the ring overlap region as in the case of 13^2-CH_2. This is in contrast with the ester methyl protons of BChlide *d* reported by Smith et al.[24] They found a pronounced difference between the two

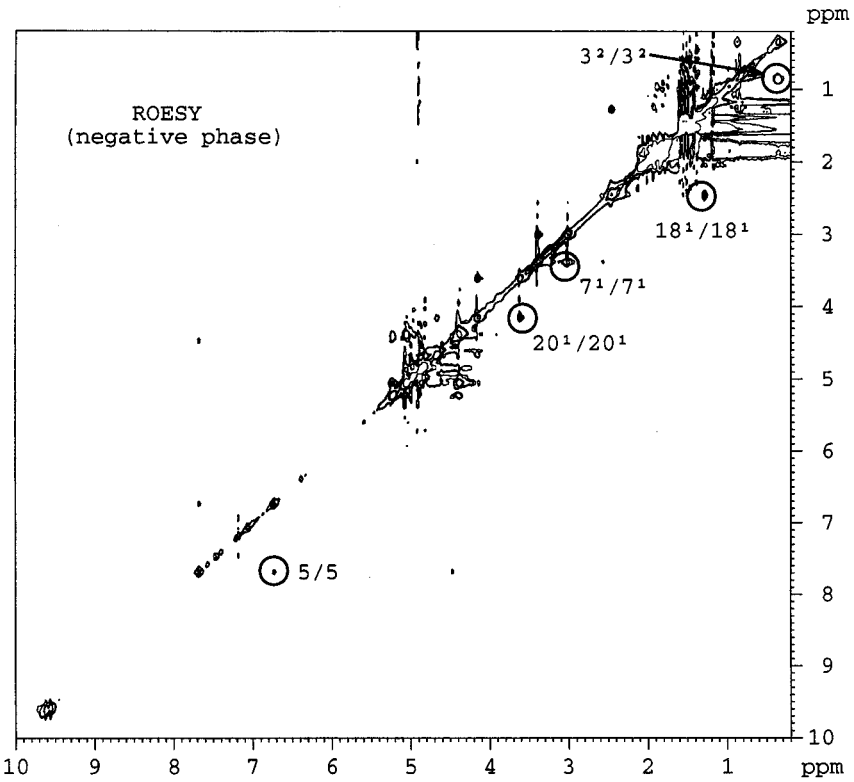

Figure 7. Negative-phase contour plot of ROESY spectrum of intact (3¹*R*)-[*E*,*E*]-BChl c_F in pure CCl_4 with a spin-lock time of 200 ms. For each t_1, 24 transients were recorded. The cross signals marked by circles were attributed to exchange between the nonequavalent protons rather than due to the NOE.

TABLE 3: Estimated Distances between Intermolecular Protons

H_i	H_j	distance (Å)
10	20^1	2.69
	2^1	3.58
20^1	5	3.76
	7^1	2.96
18^1	3^1	3.15
	7^1	3.68

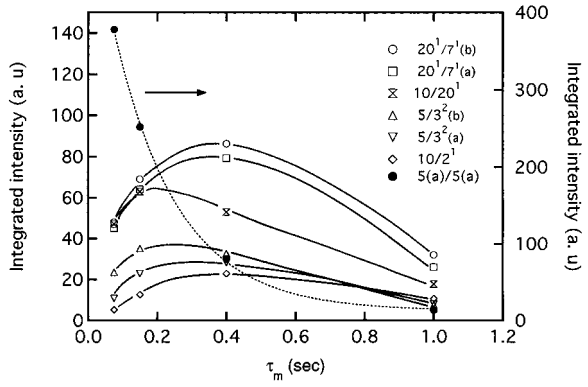

Figure 8. Variations of the integrated intensities of several selected peaks in the NOESY spectra as a function of mixing time. Only the dashed curve refers to the right scale. Open symbols represent the intensities of cross-peaks: $20^1/7^1$(b) at 3.36/4.12 ppm; $20^1/7^1$(a) at 2.98/3.59 ppm; $10/20^1$ at 3.59/9.52 ppm; $5/3^2$(b) at 0.32/6.68 ppm and $5/3^2$(a) at 0.85/7.65 ppm; $10/2^1$ at 1.20/9.52 ppm where the first chemical shift is for t_2 axis and second is for t_1 axis. Closed circles represent the intensities of the diagonal peaks of 5(a)/5(a) at 6.68/6.68 ppm.

resonances in the dimer spectrum, one sharp signal with $\Delta\delta = -0.06$ ppm and another much broader signal with $\Delta\delta = -0.62$ ppm. The different spectral shapes and complexation shifts were interpreted in terms of possible conformations of the propionic side chain in comparison with the crystal structure, leading to the conclusion that the ester chains in the two molecules adopt different conformations upon formation of BChlide *d* dimer. Considering the difference of chain length between methyl and farnesyl groups, the side chain of the [*E*,*E*]-BChl c_F dimer may adopt a different conformation from that of BChlide *d* dimer, and this could be confirmed by examining the complexation shifts of other farnesyl protons. Two resonances were observed for each of the other farnesyl protons with small downfield shifts, suggesting that the whole farnesyl side chain is not fully extended in the solution but rather adopts some conformation with most of its length close to the dimer core. This is somewhat similar to the situation reported for the BChlide *d* dimer in which an intermolecular hydrogen bond was assumed between the carbonyl of the lower molecule and the hydroxyl of the upper molecule with the propionic side chain folded back over the parent molecule.[24] However, any conformation adopted by the farnesyl chain *over* the macrocyclic plane seems unlikely because in this case substantial upfield shifts could be expected for some of the farnesyl protons. Since we do not know the conformation of farnesyl chain in monomeric [*E*,*E*]-BChl c_F, our explanation at this stage is that the farnesyl side chain in the dimer may adopt a folding-back conformation with most of the tail part fluctuating around the periphery of the macrocycle in a restricted motion and the f1 methylene being positioned just at the folding point.

The NOESY pulse sequence used in this study actually measures cross-relaxation from two origins: dipolar coupling and exchange. Both of them are present in this system. The ROESY results indicate that BChl *c* molecules in the dimer experience a physical interchange between the two molecules with different configurations, i.e., the molecule at configuration A exchanges with another molecule (within the dimer or in another dimer) at configuration B. As we have identified those

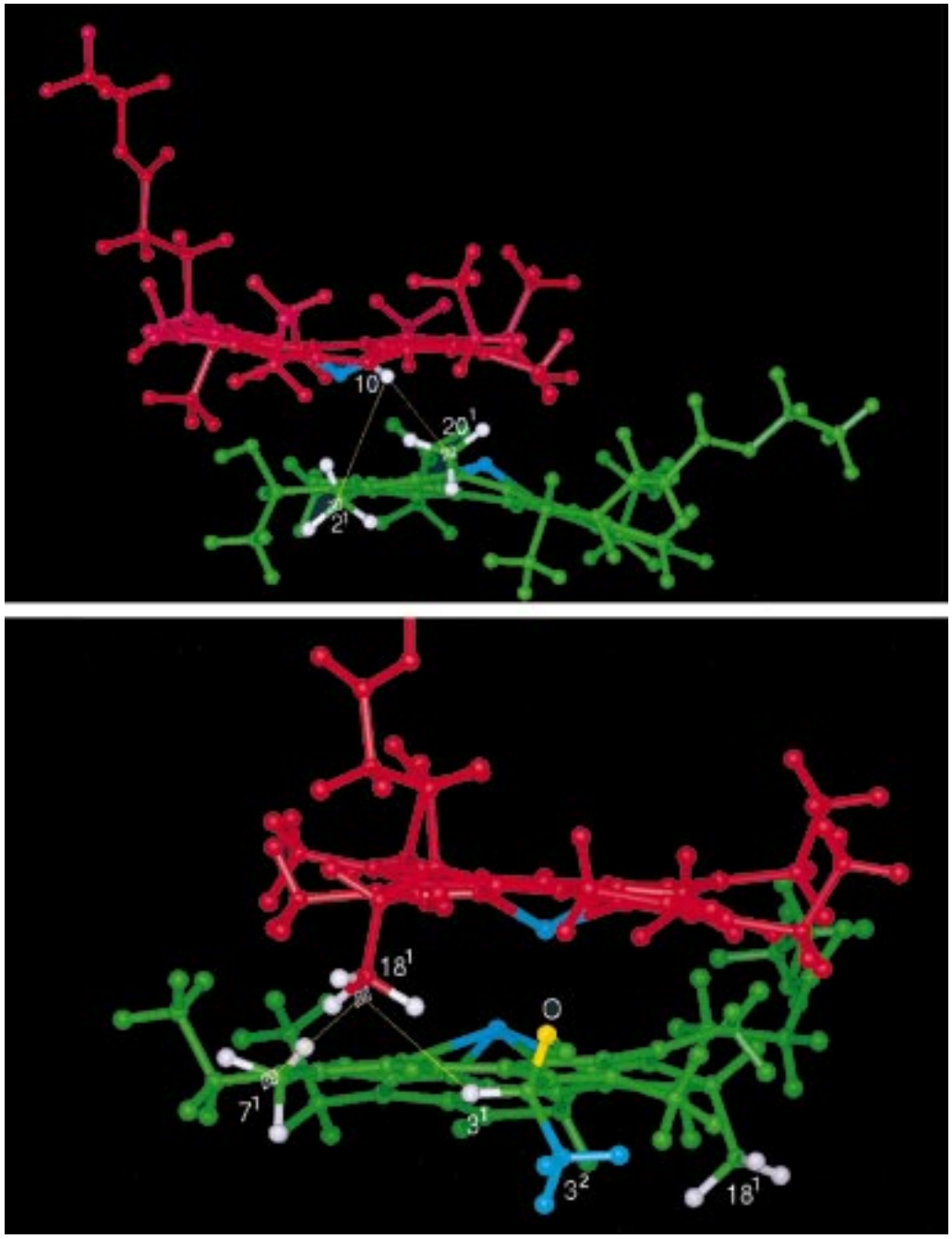

Figure 9. Side views of the BChl *c* dimer structure with an antiparallel piggy-back conformation. The energy-minimized structure was obtained by molecular mechanics calculation with six intermolecular distances determined from NOESY experiment as constraints. Farnesyl side chain was replaced by an ethyl group. Pseudoatoms (white diamonds) were introduced in the methyl groups for representing the average positions of the three protons. Part a, top, shows that the 10-proton of upper molecule (red) is in close to the 2^1- and 20^1-protons of the lower molecule (green). Part b, bottom, shows the conformation of the 3-hydroxyethyl group of the lower molecule and the close distances between 18^1-protons of the upper molecule and the 3^1- and 7^1-protons of the lower molecule. Note that the 18^1-methyl of the lower molecule points downward.

signals due to exchange, an estimation of the exchange rate may be made from the intensities of NOESY signals. For a simple two-site exchange between two uncoupled systems of spins *A* and *B*, if we assume equal populations and spin−lattice relaxation time $T_{1,A} = T_{1,B} = T_1$, then the exchange rate constant, $k = k_{AB} + k_{BA}$, can be calculated using the intensities of diagonal peaks (I_{AA}, I_{BB}) and cross-peaks (I_{AB}, I_{BA}) as follows:[57]

$$k = \frac{1}{\tau_m} \ln \frac{r+1}{r-1} \qquad (1)$$

where $r = (I_{AA} + I_{BB})/(I_{AB} + I_{BA})$. Applying the equation to the NOESY data of [*E*,*E*]-BChl c_F in CCl_4 yielded $k = 1.8-1.9$ s^{-1} over a range of $\tau_m = 0.075-1.0$ s. The extremely small exchange rate constant is not surprising in view of the reduced molecular motion resulting from the formation of dimer and the increased viscosity of CCl_4 (viscosity ratio $\eta(CCl_4)/\eta(CH_3OH) = 1.59$ at 20 °C). The two sets of well-resolved resonances and negative NOE effects observed in the [*E*,*E*]-BChl c_F dimer spectra were also a consequence of the slow exchange.

The complete assignment of all the peripheral proton resonances together with quantitative NOE measurements provides unambiguous evidence for the macrocyclic geometry. The strong intermolecular NOE signals observed for 10-H/20^1-H and 10-H/2^1-H pairs immediately excluded the face-to-face configura-

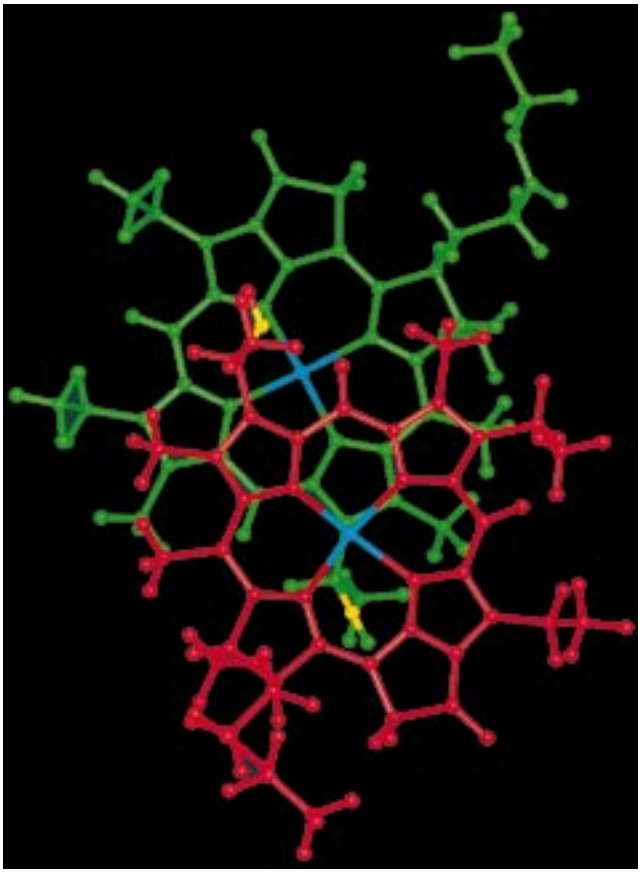

Figure 10. Top view of the BChl *c* dimer showing the overlap of the macrocycles. The structure is the same as in Figure 9. Hydroxyethyl groups and 5-protons fall entirely within the macrocycle of the adjacent molecule. Magnesium and hydroxyl oxygen atoms are blue and yellow, respectively.

tion and led to an antiparallel piggy-back dimer conformation. This is in agreement with the conclusion reached by ring current calculation that the piggy-back model best satisfied the NMR data for the BChlide *d* dimer structure in solution, even though the face-to-face arrangement was shown to be also computationally compatible with the observed shifts.[24] The dimer structure determined for BChl *c* showed plane-to-plane distances of 3.2−3.4 Å, indicating a close interaction between the two macrocyclic planes. Kratky and Dunitz reported a similar value of about 3.6 Å from X-ray crystallographic data for methyl chlorophyllide dihydrate with one-dimensional stacks of partially overlapped rings.[58] Calculation from the ring current model by Smith et al. also gave an average separation of about 3.5 Å between the parallel planes for BChlide *d* dimer.[24] Owing to the large overlap determined between the macrocycles, the hydroxyethyl groups were found to be put over ring III of the adjacent molecules with the oxygen atom apart from a position along the perpendicular direction through the central Mg (Figure 10). This is in contrast to the crystallographic results for the chlorophyll derivatives in which the oxygen atom of a water molecule is coordinated to the Mg atom in an almost vertical direction.[58,59] The difference in coordination may be interpreted in terms of the differences between a water molecule and the macrocycle-attached hydroxyethyl group for which large conformational restrictions could be expected. The Mg···O distances were measured to be about 2.9 Å, similar to that estimated for the BChlide *d* dimer. The configuration of the hydroxyethyl groups, with dihedral angles to chlorin planes (OCCC) of 45° and 70°, is demonstrated to best fit the spatial environment for the *R*-type [*E*,*E*]-BChl c_F dimer. This may explain the chirality

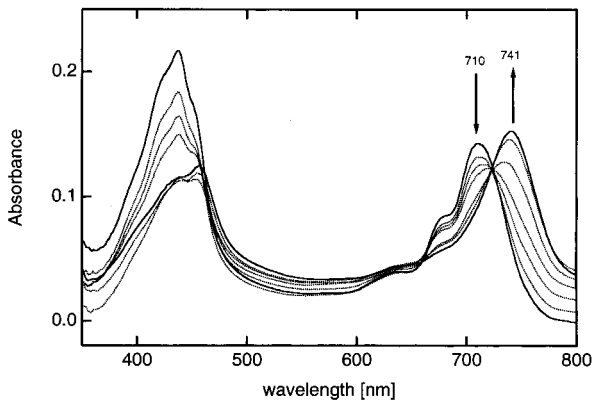

Figure 11. Time variation of absorption spectra of the intact (3^1R)-[*E*,*E*]-BChl c_F in pure CCl_4 during a drying process. The spectra were measured by a time-resolved multichannel photodiode array detector (MCPD-2000, Otsuka Electronics, Japan) with a minimum sampling time of 0.56 s and wavelength resolution of 1 nm. Sample solution of 50 μL (0.7 mM) was placed on an open, flat quartz cell (10 mm × 20 mm × 10 mm) to allow evaporation of the solvent at a natural rate at room temperature. Incident light was led from the light source by an optical fiber (12 mm i.d. and 1 m length) to the cell top, and the spectrometer was attached to the cell-bottom face. The spectra plotted in the figure were collected at 0, 5, 10, 15, 23, 30, and 33 s after the spectrum started to change. The arrows show the direction of the change.

dependence of the aggregation behavior observed for various BChl *c* and BChl *d* homologues. It has become clear that *S*-type Mg−BChl *c* and *S*-type Mg−BChl *d* fail to form stable 710 nm species in solution. Instead, they form larger heterogeneous aggregates with Q_y absorption maxima of >740 nm.[11,18] Because the positions of 3^2-methyl and 3^1-H are reversed for the *S*-configuration (see Figure 9, bottom), an antiparallel piggy-back conformation would lead to either of two consequences: (A) considerable steric congestion between the 3^2-methyl and 5-H in the same molecule and between 3^2-methyl and 18^1-methyl of the adjacent molecule if the hydroxyl group remains at the same position as shown in Figure 9b; (B) an increase in the Mg···O distance if the dihedral angle (OCCC) rotates to make the 3^2-methyl group point outward from the dimer. Obviously, either situation could destabilize the dimer structure. This implies that if a structural unit of *S*-BChl *c* and *S*-BChl *d* aggregates exists, it might adopt a different conformation from the antiparallel piggy-back structure. The stereochemical inference has been supported by a recent result on zinc bacteriopheophorbides *d*.[60]

Finally, we consider possible relationships among the 680, 710, and 740 nm species. From the results of this study along with those from ^{13}C and ^{15}N NMR[41] and small-angle neutron scattering experiments,[27] the 710-nm-rich species is obviously predominated by BChl *c* dimer with individual molecules exchanging their configurations between each other. As a result, the 680 nm species may be explained as an intermediate product of the exchange between monomer (668 nm) and dimer (710 nm). Additional evidence supports such an interpretation: (1) the 680 and 710 nm components almost always appear together in absorption spectra and the 680-nm-rich species cannot be obtained at high concentration; (2) the 680 nm component seems to be CD-inactive; (3) the 680-nm-rich species gives featureless ^1H NMR spectrum with very low signal-to-noise ratio, probably due to fast exchange. So far, the 710 nm species has been thought to be too stable to associate with each other to form higher aggregates. However, under certain conditions, formation of the 740 nm species can be observed from a system containing 710-nm-rich species. Figure 11 shows the time variation of

absorption spectra obtained from a drying process of *R*-type [*E*,*E*]-BChl c_F in CCl_4 (for experimental details, see figure caption). A clear isosbestic point can be seen between the 710 and 741 nm absorption maxima, indicating a conversion from a 710 nm species to a 740 nm species upon depletion of the solvent. The conversion might be accompanied by a conformational change of molecules in the dimer, which needs to be confirmed, but any significant change would involve a much higher energy process and is considered to be difficult in view of the extremely high stability of the dimer. A better explanation may be that the 740 nm species of *R*-type [*E*,*E*]-BChl c_F could be made up by the 710 nm species as a building unit with the conformation proposed in this study, but the association of 710 nm dimers to higher aggregates probably involves a different type of interaction responsible for holding a number of the dimers together; the interaction is considered to be much weaker than that in the dimer. Although several models have been proposed, the structure of the 740 nm species is still little known because of lack of convincing experimental results, and controversy still remains over the orientation and stacking form of the pigment molecules in the aggregates.[10,22,23] This situation may be attributed to the heterogeneous nature of the 740 nm samples formed in vitro, as can be judged from the broadness of the Q_y absorption band and by the fact that there are no diffractions observed from the samples prepared by the usual hexane treatment (data not shown). To obtain more detailed information on the structure of the 740 nm species, structurally homogeneous and highly ordered samples are thought to be a prerequisite, and as an essential step, the formation process of both *R*- and *S*-type 740 nm species needs to be well controlled and thoroughly investigated. Several such experiments are currently in progress in this laboratory.

Acknowledgment. This work was supported by a Grant-in-Aid from the Ministry of Education, Science and Culture, Japan (Nos.: 07750872, 08455377).

Glossary

BChl	bacteriochlorophyll
BChlide	bacteriochlorophyllide
Chl	chlorophyll
DQF-COSY	double quantum filtered correlation spectroscopy
NOE	nuclear Overhauser effect
NOESY	nuclear Overhauser enhancement and exchange
ROESY	rotating frame nuclear Overhauser effect
HMQC	heteronuclear multiple-quantum coherence

References and Notes

(1) Pierson, B. K.; Castenholz, R. W. *Arch. Microbiol.* **1974**, *100*, 283.
(2) Olson, J. M. *Biochim. Biophys. Acta* **1980**, *594*, 33.
(3) Blankenship, R. E.; Olson, J. M.; Miller, M. In *Anoxygenic Photosynthetic Bacteria*; Blankenship, R. E., Madigan, M. T., Bauer, C. E., Eds.; Kluwer Academic Publishers: Dordrecht, 1995; p 399.
(4) Wang, Z.-Y.; Marx, G.; Umetsu, M.; Kobayashi, M.; Mimuro, M.; Nozawa, T. *Biochim. Biophys. Acta* **1995**, *1232*, 187.
(5) Feick, R. G.; Fuller, R. C. *Biochemistry* **1984**, *23*, 3693.
(6) Chung, S.; Frank, G.; Zuber, H.; Bryrant, D. A. *Photosynth. Res*. **1994**, *41*, 261.
(7) Schmidt, K. *Arch. Microbiol.* **1980**, *124*, 21.
(8) Brune, D. C.; Nozawa, T.; Blankenship, R. E. *Biochemistry* **1986**, *26*, 8644.
(9) Nozawa, T.; Ohtomo, K.; Suzuki, M.; Morishita, Y.; Madigan, M. T. *Bull. Chem. Soc. Jpn*. **1993**, *66*, 231.
(10) Nozawa, T.; Ohtomo, K.; Suzuki, M.; Nakagawa, H.; Shikama, Y.; Konami, H.; Wang, Z.-Y. *Photosynth. Res.* **1994**, *41*, 211.
(11) Chiefari, J.; Griebenow, K.; Balaban, T. S.; Holzwarth, A. R.; Schaffner, K. *J. Phys. Chem*. **1995**, *99*, 1357.
(12) Holzwarth, A. R.; Griebenow, K.; Schaffner, K. *Z. Naturforsch.* **1990**, *45c*, 203.
(13) Griebenow, K.; Holzwarth, A. R.; van Mourik, F.; van Grondelle, R. *Biochim. Biophys. Acta* **1991**, *1058*, 194.
(14) Niedermeier, G.; Sheer, H.; Feick, R. G. *Eur. J. Biochem.* **1992**, *204*, 685.
(15) Lehmann, R. P.; Brunisholz, R. A.; Zuber, H. *Photosynth. Res.* **1994**, *41*, 165.
(16) Bystrova, M. I.; Mal'gosheva, I. N.; Krasnovskii, A. A. *Mol. Biol.* **1979**, *13*, 582.
(17) Smith, K. M.; Kehres, L. A.; Fajer, J. *J. Am. Chem. Soc*. **1983**, *105*, 1387.
(18) Olson, J. M.; Pedersen, J. P. *Photosynth. Res*. **1990**, *25*, 25.
(19) Olson, J. M.; Cox, R. P. *Photosynth. Res.* **1991**, *30*, 35.
(20) Causgrove, T. P.; Cheng, P.; Brune, D. C.; Blankenship, R. E. *J. Phys. Chem*. **1993**, *97*, 5519.
(21) Hildebrandt, P.; Tamiaki, H.; Holzwarth, A. R.; Schaffner, K. *J. Phys. Chem*. **1994**, *98*, 2192.
(22) Balaban, T. S.; Holzwarth, A. R.; Schaffner, K.; Boender, G.-J.; de Groot, H. J. M. *Biochemistry* **1995**, *34*, 15259.
(23) Mizoguchi, T.; Sakamoto, S.; Koyama, Y.; Ogura, K.; Inagaki, F. *Photochem. Photobiol.* **1998**, *67*, 239.
(24) Smith, K. M.; Bobe, F. W.; Goff, D. A.; Abraham, R. J. *J. Am. Chem. Soc.* **1986**, *108*, 1111. Abraham, R. J.; Smith, K. M.; Goff, D. A.; Bobe, F. W. *J. Am. Chem. Soc*. **1985**, *107*, 1085.
(25) Abraham, R. J.; Fell, S. C. M.; Smith, K. M. *Org. Magn. Chem*. **1977**, *9*, 367.
(26) Abraham, R. J.; Smith, K. M. *J. Am. Chem. Soc*. **1983**, *105*, 5734.
(27) Wang, Z.-Y.; Umetsu, M.; Yoza, K.; Kobayashi, M.; Imai, M.; Matsushita, Y.; Niimura, N.; Nozawa, T. *Biochim. Biophys. Acta* **1997** *1320*, 73.
(28) Smith, K. M.; Craig, G. W.; Kehres, L. A.; Pfennig, N. *J. Chromatogr*. **1983**, *281*, 209.
(29) Sato, H.; Uehara, K.; Ishii, T.; Ozaki, Y. *Biochemistry* **1995**, *34*, 7854.
(30) Senge, M. O.; Smith, K. M. *Photochem. Photobiol*. **1994**, *60*, 139.
(31) Bobe, F. W.; Pfennig, N.; Swanson, K. L.; Smith, K. M. *Biochemistry* **1990**, *29*, 4340. Huster, M. S.; Smith, K. M. *Biochemistry* **1990**, *29*, 4348.
(32) Senge, M. O.; Smith, N. W.; Smith, K. M. *Inorg. Chem*. **1993**, *32*, 1259.
(33) Davis, A. L.; Laue, E. D.; Keeler, J.; Moskau, D.; Lohman, J. *J. Magn. Reson.* **1991**, *94*, 637.
(34) Jeener, J.; Meier, B. H.; Bachmann, P.; Ernst, R. R. *J. Chem. Phys.* **1979**, *71*, 4546.
(35) Bax, A.; Davis, D. G. *J. Magn. Reson.* **1985**, *63*, 207.
(36) Hurd, R. E.; John, B. K. *J. Magn. Reson.* **1991**, *91*, 648.
(37) Shaka, A. J.; Barker, P. B.; Freeman, R. *J. Magn. Reson.* **1985**, *64*, 547.
(38) Redfield, A. G.; Kunz, S. D. *J. Magn. Reson.* **1975**, *19*, 250.
(39) Allinger, N. L. *J. Am. Chem. Soc.* **1977**, *99*, 8127.
(40) Shelnutt, J. A.; Medforth, C. T.; Berker, M. D.; Barkigia, K. M.; Smith, K. M. *J. Am. Chem. Soc*. **1991**, *113*, 4077.
(41) Wang, Z.-Y.; Umetsu, M.; Kobayashi, M.; Nozawa, T. Manuscript in preparation.
(42) Strouse, C. E.; Kollman, V. H.; Matwiyoff, N. A. *Biochem. Biophys. Res. Commun.* **1972**, *46*, 328.
(43) Goodman, R. A.; Oldfield, E.; Allerband, A. *J. Am. Chem. Soc.* **1973**, *95*, 7553.
(44) Boxer, S. G.; Closs, G. L.; Katz, J. J. *J. Am. Chem. Soc.* **1974**, *96*, 7058.
(45) Abraham, R. J.; Hawkes, G. E.; Smith, K. M. *J. Chem. Soc., Perkin Trans. 2* **1974**, 627.
(46) Lincoln, D. N.; Wray, V.; Brockmann, jun. H.; Trowitzsch, W. *J. Chem. Soc. Perkin Trans. 2* **1974**, 1920.
(47) Smith, K. M.; Unsworth, J. F. *Tetrahedron* **1975**, *31*, 367.
(48) Wray, V.; Jürgens, U.; Brockmann, H., Jr. *Tetrahedron* **1979**, *35*, 2275.
(49) Smith, K. M.; Bushell, M. J.; Rimmer, J.; Unsworth, J. F. *J. Am. Chem. Soc.* **1980**, *102*, 2437.
(50) Lötjönen, S.; Hynninen, P. H. *Org. Magn. Reson.* **1981**, *16*, 304.
(51) Bovey, F. A. In *Nuclear Magnetic Resonance Spectroscopy*, 2nd ed.; Academic Press: San Diego, 1988; pp 193, 607.
(52) Smith, K. M.; Goff, D. A.; Abraham, R. J. *Tetrahedron Lett*. **1981**, *22*, 4873.
(53) Smith, K. M.; Goff, D. A.; Abraham, R. J. *Org. Magn. Reson*. **1984**, *22*, 779.
(54) Ernst, R. R.; Bodenhausen, G.; Wokaun, A. In *Principles of Nuclear Magnetic Resonance in One and Two Dimensions*; Clarendon Press: Oxford, 1990; Chapter 9.

(55) (a) Dougherty, R. C.; Strain, H. H.; Katz, J. J. *J. Am. Chem. Soc.* **1965**, *87*, 104. (b) Katz, J. J.; Thomas, M. R.; Crespi, H. L.; Strain, H. H. *J. Am. Chem. Soc.* **1961**, *83*, 4180. (c) Woodward, R. B.; Skaric, V. *J. Am. Chem. Soc.* **1961**, *83*, 4676.

(56) Hynninen, P.; Lötjönen, S. *Synthesis* **1983**, 705.

(57) Evans, J. N. S. *Biomolecular NMR Spectroscopy*; Oxford University Press: Oxford, 1995; Chapter 1.

(58) Kratky, C.; Dunitz, J. D. *J. Mol. Biol.* **1977**, *113*, 431; *Acta Crystallogr.* **1977**, *B33*, 545.

(59) Chow, H.-C.; Serlin, R.; Strouse, C. E. *J. Am. Chem. Soc.* **1975**, *97*, 7230.

(60) Balaban, T. S.; Tamiaki, H.; Holzwarth, A. R.; Schaffner, K. *J. Phys. Chem.* **1997**, *B101*, 3424.